HHS Public Access

Author manuscript

Neuropathol Appl Neurobiol. Author manuscript; available in PMC 2017 December 01.

Published in final edited form as:

Neuropathol Appl Neurobiol. 2016 December ; 42(7): 621–638. doi:10.1111/nan.12337.

Human adult neurogenesis across the ages: An immunohistochemical study

CV Dennis, B Med Sci (Hons)[1], **LS Suh, B Sci (Hons)**[1,2], **ML Rodriguez, MBBS, FRCPA**[1], **JJ Kril, PhD**[1], and **GT Sutherland, PhD**[1]

[1]Discipline of Pathology, Sydney Medical School, University of Sydney, Camperdown, NSW 2006, Australia

[2]Dementia Research Unit, School of Medical Sciences, University of New South Wales, Kensington, NSW 2052, Australia

Abstract

Aims—Neurogenesis in the postnatal human brain occurs in two neurogenic niches; the subventricular zone (SVZ) in the wall of the lateral ventricles and the subgranular zone of the hippocampus (SGZ). The extent to which this physiological process continues into adulthood is an area of ongoing research. This study aimed to characterise markers of cell proliferation and assess the efficacy of antibodies used to identify neurogenesis in both neurogenic niches of the human brain.

Methods—Cell proliferation and neurogenesis were simultaneously examined in the SVZ and SGZ of 23 individuals aged 0.2–59 years using immunohistochemistry and immunofluorescence in combination with unbiased stereology.

Results—There was a marked decline in proliferating cells in both neurogenic niches in early infancy with levels reaching those seen in the adjacent parenchyma by four and one year of age, in the SVZ and SGZ, respectively. Furthermore, the phenotype of these proliferating cells in both niches changed with age. In infants, proliferating cells co-expressed neural progenitor (epidermal growth factor receptor), immature neuronal (doublecortin and beta III tubulin) and oligodendrocytic (Olig2) markers. However, after three years of age, microglia were the only proliferating cells found in either niche or in the adjacent parenchyma.

Conclusions—This study demonstrates a marked decline in neurogenesis in both neurogenic niches in early childhood, and that the sparse proliferating cells in the adult brain are largely microglia.

Keywords

adult neurogenesis; human postmortem brain tissue; immunohistochemistry; microglial proliferation; subventricular zone and subgranular zone

Corresponding author: Greg Sutherland, Discipline of Pathology, Rm 6211 Level 6W, Charles Perkins Centre D17, University of Sydney, NSW 2006, Australia; Tel +61 2 90367233; Fax +61 2 86271601; g.sutherland@sydney.edu.au.

Statement of Conflict of Interest

None of the authors have any conflict of interest in respect of the manuscript contents.

Introduction

It has been proposed that enhancement of endogenous neurogenesis using pharmaceutical or environmental measures could be an effective therapeutic strategy for neurodegenerative diseases [1, 2]. The ultimate success of these efforts would appear to be predicated on there being sufficient levels of neurogenesis in the aged human brain to respond to manipulation. The prolificity of adult neurogenesis in all mammals declines with age [3] although the timing of this and the extent to which it occurs in the human brain remains the subject of considerable debate.

There are two major neurogenic niches in the adult human brain, the subventricular zone (SVZ) underlying the wall of the lateral ventricles and the subgranular zone (SGZ) in the dentate gyrus of the hippocampus. In both niches, pluripotent neural stem cells give rise to transit amplifier cells that differentiate into neuroblasts, astrocytes and oligodendrocyte precursor cells [3]. Studies in various lower mammals have shown that neuroblasts from the SVZ migrate, via the rostral migratory stream (RMS), and integrate as interneurons into the granule cell layer of the olfactory bulb where they are thought to modulate olfactory learning and performance [4, 5]. In contrast, neuroblasts from the SGZ migrate a short distance to the adjacent granule cell layer (GCL) [6] where survivors are thought to facilitate the temporal separation of spatial memories [7].

In pioneering work Curtis and colleagues used immunohistochemistry to identify the endogenous proliferation marker, proliferating cell nuclear antigen (PCNA), to demonstrate the presence of a functional RMS in humans [8]. In contrast, Sanai and colleagues used an alternative proliferation marker, Ki67 and the immature neuronal marker doublecortin (DCX) [9] to show that SVZ neurogenesis and migration along the RMS ceased by two years of age [10]. Knoth and colleagues used DCX and PCNA to demonstrate residual neurogenesis in the SGZ in adults up to 100 years of age [11]. To our knowledge no study has explored proliferation in the human SGZ using Ki67 across a wide age range.

More recently an alternative methodology, radioactive carbon dating of neuronal DNA, has shown numerous adult-born neurons in the adult human hippocampus [12] and the SVZ [13], although the neuroblasts produced by the latter appear to migrate into the adjacent caudate nucleus [13] rather than entering the olfactory bulb via the RMS [14]. One of the major advantages of this technique is that unambiguous confirmation of proliferating cell fate can be confirmed using mature cell markers such as the neuronal marker, NeuN. However the technique is limited to one or two specialist laboratories, worldwide.

Notwithstanding the contribution of radioactive carbon dating to this area, immunohistochemistry remains a much more accessible technique, although findings to date on the extent of adult neurogenesis have been marker-dependent. In an attempt to clarify the true extent of neurogenesis in both niches of the human brain we have compared and contrasted Ki67, PCNA and DCX immunostaining of postmortem tissue across a range of ages.

Materials and methods

Cases

This project was conducted following approval from the Human Research Ethics Committee of the University of Sydney (HREC #13027). Formalin-fixed paraffin-embedded (FFPE) sections of the wall of the lateral ventricle and adjacent head of the caudate nucleus (CN) at the level of nucleus accumbens, and the hippocampus at the level of the lateral geniculate nucleus, were obtained from neurologically normal subjects (0.2 – 59 years; n = 23) (Table 1). Additional sections from the superior frontal gyrus (SFG) were also obtained from the three eldest adults (Table 1 #21 – 23). Tissue from eight individuals ≥ 24 years (adult) was obtained from the New South Wales Brain Tissue Resource Centre (NSW BTRC). Tissue from 15 individuals ≤16 years (juvenile), including 11 ≤4 years (infant), were obtained from the NSW Department of Forensic Medicine. Adult and juvenile tissues were fixed in 15 and 20% formalin, respectively, for 2–3 weeks, followed by paraffin embedding. NSW BTRC provided information on age, gender, postmortem interval (PMI), cause of death, brain pH, alcohol intake and liver pathology. Only age, PMI, gender and the cause of death were available for the remainder of cases (Table 1).

Immunohistochemistry

7μm FFPE sections were dewaxed through graded alcohols prior to antigen retrieval and immunostaining. Antigen retrieval was performed in a decloaking chamber (BioCare medical DC2002, Concord, USA) for 30 minutes at 95°C using 10 mM Tris/1 mM EDTA buffer pH 9.0. A higher maximum temperature of 110°C was necessary for antigen retrieval for Ki67 due to its greater susceptibility to the effects of fixation [15]. Sections were washed in 0.05M Tris/0.015M NaCl/0.05% Tween-20 (TBST, pH 7.4) and incubated for 10 minutes in 3% H_2O_2 in methanol, followed by 15 minutes in 10% normal horse serum (NHS) before overnight incubation with the following primary antibodies at 4°C: Ki67 (Clone MIB-1; mouse monoclonal, 1:500; M7240, Dako, Denmark), doublecortin (DCX; goat polyclonal, 1:500, sc-8066, Santa Cruz Biotechnology, California) or PCNA (Clone PC10, mouse monoclonal, 1:500, sc-56, Santa Cruz Biotechnology). Primary and secondary antibodies were diluted in 1% NHS prepared in TBST. The slides were incubated in the secondary antibody (1:200; biotinylated anti-mouse BA-2000 and biotinylated anti-rabbit BA-1000, Vector Laboratories, Meadowbrook, Queensland) for 30 minutes, then with an avidin-biotin-peroxidase complex (1:100; PK-6100, Vector Laboratories) for 30 minutes. Negative controls, omitting the primary or secondary antibody, were run concurrently for all antibodies. Visualisation was with DAB in 5% H_2O_2 for 2–3 minutes followed by hematoxylin counterstaining.

Immunofluorescence

Immunofluorescence co-localisation studies with cell specific markers were performed using the same antigen retrieval protocol outlined above. Sections were then washed in 0.01M phosphate buffered saline (Bioline, Alexandria, Australia) with 0.1% Tween-20 (PBST), blocked for 20 minutes in 10% NHS and incubated overnight at 4°C in a primary antibody cocktail containing up to three antibodies raised in different species including: Ki67; DCX; PCNA; beta III tubulin (rabbit polyclonal, 1:200, ab18207, Abcam, Waterloo, NSW),

ionized calcium binding adaptor molecule 1 (Iba1, rabbit polyclonal, 1:1000; 019-19741, Wako Pure Chemicals, Osaka, Japan), glial fibrillary acidic protein (GFAP, rabbit polyclonal, 1:200; Z0334, Dako, Denmark), epidermal growth factor receptor (EGFR, rabbit monoclonal, 1:200; 04-338, Merck Millipore, Billerica, USA) and oligodendrocyte lineage transcription factor 2 (Olig2, clone ERP2673 1:200; ab109186, Abcam). The sections were protected from UV light and incubated in a secondary antibody cocktail (1:200: AlexaFluor 488, donkey anti-goat IgG, A10055; AlexaFluor 568, donkey anti-mouse IgG, A10037; AlexaFluor 647, donkey anti-rabbit IgG, A31573) for 30 minutes. Tissue autofluorescence was quenched using 0.1% Sudan black B (B.D.H Laboratory Chemicals Group, United Kingdom) in 70% ethanol for 4 minutes. Sections were then cover slipped using ProLong® Gold Antifade Reagent with DAPI (P36935, Life Technologies, Mulgrave, Victoria) and left for 24 hours at room temperature, sealed with nail polish and stored at 4°C. Images were then obtained using confocal microscopy (Zeiss LSM 510 META Spectral microscope) at the Advanced Microscope Facility of the Bosch Institute (University of Sydney).

Stereological quantification

$Ki67^+$, DCX^+ and $PCNA^+$ cells were counted within the entire SVZ and SGZ of each section using an Olympus BX53 microscope equipped with StereoInvestigator (v5.65). The SVZ was defined as the tissue extending from the ependymal layer (layer I) to the medial margin of the head of the CN which is delineated by a distinct myelin layer (layer IV) [16, 17]. Accordingly, all immunopositive cells in the SVZ were counted within the hypocellular layer (layer II) and the adjacent layer containing a ribbon of astrocyte cell bodies (layer III) [17] (Fig. S1A). As newborn neurons can migrate across the width of the GCL, the SGZ was arbitrarily defined as extending from the junction of the GCL and the molecular layer to the boundary between the polymorphic layer and the CA4 subregion of the hippocampus (the latter defined by the presence of pyramidal neurons) (Fig. S1B). The “Meander Scan” function was used at 40x magnification and immunopositive cells were recorded manually at each scan site. After the meander scan had sampled the entire area of interest, the area scanned and the total number of immunopositive cells counted were recorded and cell density calculated (cells/mm^2).

$Ki67^+$ cells were also counted in the SFG of three neurologically normal adults using unbiased stereology. Cortical ribbons were outlined using a 4x objective and then randomly sampled using the optical dissector probe function of the software. Counts were then performed at 40x magnification with a meander sampling rate of 1% and a counting frame of 22,500 μm^2.

Images of the proximal RMS were obtained using a slide scanning microscope (Zeiss Axio Scan.Z1, Gena, Germany). Using Zen imaging software (v1.1.2.0, 2012 Blue Edition, Gena, Germany) the RMS was outlined prior to scanning and images, taken at 100x magnification, stitched together and exported.

Confocal fluorescence microscopy was used to phenotype $Ki67^+$ cells throughout the SVZ and SGZ of seven individuals (six juveniles including five infants). Neurogenic events were explored by triple staining with Ki67 and DCX and either EGFR (a putative transit amplifier cell marker) [18] or beta III tubulin (an immature neuronal marker) [19]. To determine the

overall composition of proliferating cells, sections were triple-stained with Ki67, DCX and either GFAP (a mature astrocyte marker [20, 21], Iba1 (microglial marker) [22, 23] or Olig2 (an oligodendrocytic lineage marker) [24, 25]. Fluorescent images were imported using LSM Image Browser v3.5 (Zeiss) and $Ki67^+$ cells were scored as positive or negative for DCX and the cell-specific markers by an investigator blinded to case status (CD).

Statistical analysis

Statistical analyses were performed using the statistical software package GraphPad Prism 6 (v6.0d, GraphPad Software, Inc. 2013). Juvenile versus adult group differences were assessed using a Student's t-test. A ratio-paired t-test was used to compare the relative densities of markers across all individuals. The relationships between markers and age were evaluated by Pearson correlation. The level of significance was chosen at $p = 0.05$ for all tests.

Results

Baseline proliferation in the adult human brain

The baseline level of cell proliferation in the adult brain outside the neurogenic niches was determined by counting $Ki67^+$ cells in the SFG and the CN of three adults. $Ki67^+$ cells were identified in all cases (mean density 2.9 ± 2.1 cells/mm^2) and our previous work has shown these cells to be almost exclusively microglia [23]. No DCX^+ cells were identified in the CN.

Markers of proliferation and neurogenesis in the subventricular zone

$Ki67^+$ cells, exclusively with nuclear staining, were distributed uniformly along the SVZ at all ages (Fig. 1A, C, E, G). DCX^+ cells were distributed unevenly along the SVZ, often present as aggregates (Fig. 1B and D). DCX staining varied with age, being somatic (perinuclear), dendritic (processes) or a combination of both in individuals ≤ 4 years of age, predominantly somatic in 7–16 year olds (Fig. 1B, D, F) and absent in individuals older than 16 (Fig. 1H).

$PCNA^+$ cells were distributed uniformly along the SVZ in all individuals. Staining was nuclear but varied considerably in intensity. PCNA staining of ependymal cell nuclei, more intense in adults, was seen in all cases. There was no staining of ependymal cells with either Ki67 or DCX (Fig. S2).

Proliferating cells in the human subventricular zone decline with age

There was a marked decrease in cell proliferation in the infant SVZ (Fig. 1). The density of $Ki67^+$ cells decreased dramatically over the first year of life and by four years of age was similar to the density in adult SFG and CN (2.6 cells/mm^2) (Fig. S3).

Similarly, the density and total number of DCX^+ cells in the SVZ declined with age. DCX^+ cell density declined from 234.1 cells/mm^2 in the youngest individuals (0.2 year-old) to 4.6 cells/mm^2 in the 16 year old, although the highest density was seen in a three year-old

(391.2 cells/mm^2). DCX$^+$ cells were not identified in individuals older than 16 years (Fig. S3).

There was a positive correlation between Ki67$^+$ and DCX$^+$ cell densities in the juvenile SVZ ($r^2 = 0.39$; $p = 0.014$) with DCX$^+$ cells exceeding Ki67$^+$ cells in 13/15 cases (mean = 2.6 fold; 95% CI = 1.7 – 4.2)(Fig. S3).

The density of PCNA$^+$ cells was greater than the density of Ki67$^+$ cells in juvenile cases (mean = 3.9 fold; 95% CI = 1.8–8.5, $p = 0.002$). However, unlike Ki67$^+$ and DCX$^+$ cells, the PCNA$^+$ cell density did not correlate with age (Fig. S3). The density of PCNA$^+$ cells in adults (mean = 421.3 ± 121.1, range 0.76–799.3 cells/mm^2, n = 8) was significantly higher than in juveniles (mean = 124.3 ± 26.0, range = 14.7–327.0 cells/mm^2, n = 15, $p = 0.005$).

The phenotype of proliferating cells in the SVZ changes with age

Ki67$^+$ cells in the juvenile SVZ (n = 6; Table 1) variably co-labelled with DCX (Fig. 2), beta III tubulin (Fig. 2A–D), EGFR (Fig. 2E–H), Olig2 (Fig. 2I–L), and Iba1 (microglia) (Fig. 2M–P) but not GFAP (astrocytes) (Fig. 2Q–T).

The phenotype of Ki67$^+$ cells in the SVZ differed with age (Fig. 3). In the youngest individual examined by confocal microscopy (1 year) Ki67 co-localised with DCX (65%). Triple labelling showed that Ki67$^+$/DCX$^+$ cells could be further subdivided into Ki67$^+$/DCX$^+$/EGFR$^+$ (29%), Ki67$^+$/DCX$^+$/beta III tubulin$^+$ (19%) and Ki67$^+$/DCX$^+$ only (17%) cells. Additionally, there were occasional Ki67$^+$/DCX$^-$/EGFR$^+$ and Ki67$^+$/DCX$^-$/beta III tubulin$^+$ cells. The remaining Ki67$^+$ cells were either Olig2$^+$ (20%) or Iba1$^+$ (10%). In a 3.9 year-old Ki67$^+$ cells co-labelled with DCX, Olig2 or Iba1 but no Ki67$^+$/DCX$^+$/EGFR$^+$ or Ki67$^+$/DCX$^+$/beta III tubulin$^+$ cells were identified. No Ki67$^+$/DCX$^+$ cells were seen at 14 years and older with all Ki67$^+$ cells examined in the adult SVZ being Iba1$^+$ (Fig. 3). Ki67$^+$/GFAP$^+$ cells were not seen at any age.

Markers of proliferation and neurogenesis in the SGZ

In juvenile brains, Ki67$^+$ cells were common within, but not confined to, the SGZ. Ki67$^+$ cells were also found in the molecular layer of the dentate gyrus and in the CA4 region of the hippocampus (Fig. 4A and C). Ki67$^+$ cells were exceptionally rare in the adult SGZ and adjacent regions (Fig. 4E and G).

The distribution and staining pattern of DCX$^+$ cells differed with age. In juveniles, DCX$^+$ cells were densely clustered within the PML near the GCL border with either somatic, dendritic or a combination of somatic and dendritic staining (Fig. 4B and D). Clustered DCX$^+$ cells were not present in cases over three years of age and only sparse DCX$^+$ cells were seen in the older juveniles and adults (2/8; Fig. 4F and H). Similar to the SVZ, nuclear PCNA staining varied in intensity and was distributed uniformly across all areas of the dentate gyrus (Fig. S2).

Proliferating cells in the human SGZ decline with age

As noted in the SVZ, there was a dramatic decline in the density of Ki67$^+$ cells in the SGZ during the first year of life. In a 0.2 and 0.3 year-old there were 17.9 and 20.6 cells/mm^2,

respectively. At one year of age, the mean density was 3.77 ± 1.39 cells/mm^2 (n = 3), similar to the Ki67$^+$ cell density in the adult SFG and CN (baseline levels) (p = 0.66; Fig. S4). Ki67$^+$ cells were only present in 2/8 adult SGZ and their mean density (0.27 ± 0.18 cells/mm^2) was lower than in the adult SFG (2.6 cells/mm^2; p = 0.006).

As in the SVZ, the density of DCX$^+$ cells exceeded that of Ki67$^+$ cells in the SGZ in 14/15 juveniles (mean ratio = 18.0, 95% CI = 6.9 – 47.0). The density of both Ki67$^+$ and DCX$^+$ cells declined with age although the decline was more rapid for Ki67$^+$. At one year of age, DCX$^+$ cells were still numerous (mean = 255 ± 81 cells/mm^2) but then either absent from, or very sparse in (n = 3, mean = 0.45 ± 0.30 cells/mm^2), the eight adults examined (Fig. S4).

The phenotype of proliferating cells in the SGZ changes with age

In the six juveniles examined (n = 6, 1–14 years) Ki67$^+$ cells in the SGZ variably co-expressed DCX, EGFR (Fig. 5A–D), Olig2 (Fig. 5E–H) and Iba1 but not beta III tubulin (Fig. 5M–P) or GFAP (Fig. 5Q–T).

In younger individuals (1 and 1.5 years) the majority of Ki67$^+$ cells co-expressed the transit-amplifier cell marker, EGFR. Ki67$^+$/DCX$^+$ and Ki67$^+$/Olig2$^+$ cells were also seen in infants up to 3.9 years. Some Ki67$^+$/DCX$^+$ cells co-expressed Olig2 but none co-expressed beta III tubulin or EGFR. In contrast to the SVZ, where 10% of Ki67$^+$ cells in juveniles co-expressed Iba1, no Ki67$^+$/Iba1$^+$ cells were identified in the SGZ < 3.9 years of age. All Ki67$^+$ cells in older individuals (14 and 54 year-olds) were Iba1$^+$ (Fig. 6).

Comparison of Ki67 and DCX in the subventricular and subgranular zones

In all cases, Ki67$^+$ cells were more numerous in the SVZ than in the SGZ, although the Ki67$^+$ cell density varied considerably between cases. In the juvenile group, the average SVZ/SGZ density ratio was 9.7 (n = 13; 95% CI = 5.9–16.0). The two cases with no Ki67$^+$ cells in the SGZ were excluded from this analysis. Since in adults, Ki67$^+$ cells were only identified in the SGZ in 2/8 cases (37 and 54 year-olds) a meaningful density ratio between the two niches could not be determined.

Rostral migratory stream

In some individuals a RMS from the rostral extremity of the frontal horn of the lateral ventricle, could be identified by its distinctive SVZ-like cytoarchitecture (greater cellularity) and the presence of epdendymal islets [10, 26]. The RMS was bordered by the CN and genu of the corpus callosum (CC) (Fig. 7 and Fig. S5). Numerous Ki67$^+$ and DCX$^+$ cells were present throughout the RMS of the youngest individual (0.2 year-old; Fig. 7A, D) but were spatially distinct. DCX$^+$ cells were seen more dorsomedially adjacent to the CC (Fig. 7A–C) while Ki67$^+$ cells were largely localised to the ventrolateral aspect of the RMS adjacent to the head of the CN (Fig. 7D–E). In the 0.2 and one year-old approximately 15% of the DCX$^+$ cells showed colocalisation with Ki67 (Fig. 7F, G). Similar to the SVZ, there was a dramatic decline in the number of DCX$^+$ and Ki67$^+$ cells in the RMS during the first year of life with only a single DCX$^+$ cell and rare Ki67$^+$ cells seen in older individuals. In all the adults examined (n = 8, 24–59 years) there was only one case (a 54 year-old) with a single DCX$^+$ cell in the RMS (Fig. 7G) while the rare Ki67$^+$ cells seen in the adult RMS co-

localised with Iba1 (Fig. 7H). Ependymal islets were dispersed throughout the RMS at all ages. In individuals younger than 2.5 years there were DCX^+ and $Ki67^+$ cells (Fig. S5 D–F) both within (non-patent) and surrounding the islets.

In contrast to Ki67 and DCX, the majority of RMS cells in all cases including ependymal cells of the ependymal islets were immunopositive for PCNA (Fig. S5A–C). Furthermore, in the infant brains PCNA staining was at two distinct intensities, a small subgroup of intensely stained cells with a similar density and distribution to the $Ki67^+$ cells, and the majority of $PCNA^+$ cells, including ependymal cells, that were moderately stained (Fig. S5A, B). In older brains intensely staining $PCNA^+$ cells were rare, paralleling the density and distribution of $Ki67^+$ cells, while the moderately staining population remained (a 54 year-old; Figure S5C).

Discussion

The potential benefits of therapeutically manipulating endogenous adult neurogenesis for patients with neurodegenerative diseases are immense. Both pharmaceutical and environmental manipulation has been shown to affect adult neurogenesis in many mammalian species but successful manipulation in humans is likely to depend on there being a sufficient level of neurogenesis at the ages that these diseases are prevalent.

We had previously shown that there was no difference in cell proliferation in the SVZ of chronic alcoholics compared to neurologically normal controls [16]. In that study, and in previous studies examining the human SVZ and RMS [8, 10] the density of proliferative events depended on whether PCNA or Ki67 was used as a marker. Far fewer proliferating cells are identified in studies using Ki67 but epitope retrieval from fixed human brain tissue is known to be more difficult than for PCNA [15]. In order to clarify the true state of cell proliferation in adult neurogenic niches, fixed postmortem human brain tissue from neurologically normal infants to middle-aged subjects were examined. DCX was also included as an immature neuronal marker whose expression should partially overlap with both proliferative markers and confirm neurogenesis. Our results show that the density of $Ki67^+$, DCX^+ and $Ki67^+/DCX^+$ cells in the SVZ and SGZ is high prior to four and one year of age, respectively but then decreases markedly with age. In the SVZ this replicates the results of Sanai and colleagues in juveniles up to 18 months of age [10]. Furthermore the pattern of DCX^+ immunostaining in the SGZ of juveniles and adults in this study is remarkably similar to the exponential decrease with ageing described by Knoth and colleagues [11]. Again, consistent with our results, Knoth *et al.* demonstrated that there was no relationship between $PCNA^+$ and DCX^+ cell density across a wide range of ages.

$PCNA^+$ cells were more frequent than $Ki67^+$ cells both within and outside the neurogenic niches and PCNA also stained the nuclei of mature ependymal cells. This has been reported in other studies [16, 27–29] as has PCNA staining of mature leptomeningeal cells [30]. It is not clear whether staining in these non-proliferating cell populations is specific, specific but identifying a modified form of PCNA [31], or is non-specific, detecting a shared epitope on an unrelated protein. In the present study, non-specific ependymal staining due to cross reactivity with secondary anibodies was ruled out by the inclusion of a no primary antibody

negative control. Furthermore the likelihood of non-specificity was somewhat mitigated by the PCNA immunostaining pattern being seen with multiple PCNA antibodies raised in different species and from different clones (data not shown). Unlike DCX and Ki67, the majority of cells within the adult RMS were PCNA immunopositive including the ependymal islet cells. However, in the infant RMS there was a combination of this adult pattern interspersed with a few intensely stained cells. These intensely stained cells resembled the Ki67 pattern of immunopositivity and may represent the true proliferative population.

If staining in the majority of $PCNA^+$ cells is specific, then PCNA must serve a distinct function in mature cells. Roles in DNA repair or transcription have been suggested [32] and a recent study showed that there are two pools of PCNA in mammalian cells, one involved in replication and a second soluble nucleoplasmic pool of unknown function [33]. Our findings are consistent with PCNA antibodies labelling two pools of PCNA in the infant human SVZ and RMS, with only the non-proliferative pool remaining in the adult. Notwithstanding the need for further work to delineate the functional significance of moderate PCNA expression in the dentate gyrus, ependymal layer and adjacent areas, our results strongly suggests that PCNA-based IHC studies will overestimate proliferative events in human postmortem brain tissue.

Notwithstanding DCX immunostaining of human astrocytes [34] and mature murine neurons [35, 36], our findings in the SVZ and SGZ combined with those of Sanai *et al*. in the SVZ [10] suggest that within the confines of the neurogenic niches, the combination of DCX and Ki67 immunostaining gives an accurate depiction of adult neurogenesis. This conclusion is supported by studies that employed either Ki67 [37] or DCX [11] in the SGZ. These studies also reported changes in the subcellular location of DCX [11, 37]. Boekhoorn *et al*. suggested that somatic DCX staining was related to PMI [37], however Knoth and colleagues, having matched for PMI, considered that somatic staining identified the most immature progenitor cells, notwithstanding these cells being found throughout the GCL [11]. Similar to Knoth *et al*, we found that somatic DCX staining was identified throughout the GCL independent of the PMI.

Co-localisation studies enabled us to explore the changing cell phenotype in the SVZ and SGZ with age. In infants there was evidence of neurogenesis with transit-amplifier cells ($Ki67^+/DCX^+/EGFR^+$ and $Ki67^+/DCX^-/EGFR^+$) and neuroblasts ($Ki67^+/DCX^+$/beta III $tubulin^+$) in both niches consistent with previous studies [3, 38, 39] as well as oligodendrogenesis with $Ki67^+/DCX^{+/-}/Olig2^+$ cells [40]. GFAP was also expected to co-localise with Ki67 in the neurogenic niches due to the likely presence of both the GFAP-δ^+ type B (neural stem) cells [41] and newborn astrocytes [3]. The lack of co-localisation may be partially explained by a largely quiescent neural stem cell population at the ages we examined. In this respect, our findings agree with a previous study that demonstrated no $Ki67^+$/GFAP-δ^+ cells in the aged human (82 year-old) SVZ [42]. Whereas, the extent of ongoing astrogliogenesis in the adult human SVZ or SGZ, unlike in the rodent SVZ [43], is unknown.

In terms of the RMS our results are consistent with previous studies that suggested that chains of migrating neuroblasts are not seen in the human RMS after 2 years of age [10]. They are also in agreement with studies using atmospheric radioactive carbon from nuclear weapon testing that showed no evidence of adult-born neurons in the olfactory bulb [13, 14]. Ernst *et al.* suggested that SVZ-derived neurons deviated into the adjacent CN rather than continuing along the RMS to the olfactory bulb in the adult human brain [13], although our current and previous work in alcoholic and normal brains [16, 23] found no evidence of migration of proliferative cells into the CN. One caveat with our characterisation of the RMS is that it relied on a single coronal section at the level of the CN. This contrasts with more extensive analyses undertaken previously [8, 10, 26] and our findings must be considered in this context. Nevertheless, the distinct spatial separation of the majority of $Ki67^+$ and DCX^+ cells in the infant RMS suggests that proliferation, including neurogenesis, may continue along the length of the RMS rather than being confined to the SVZ [26]. A proliferative RMS has been shown in other species [44], [45], [46] and provides an alternative explanation to the traditional view that a proportion of neuroblasts remain mitotically active for their entire journey along the RMS[8].

In contrast to our findings in the SGZ, Spalding and colleagues, using atmospheric radioactive carbon techniques, suggested that human SGZ neurogenesis continues throughout life [12]. These apparently discordant results may be explained, at least in part, by differences in sampling techniques. Firstly Spalding *et al.* homogenised the entire hippocampus, approximately 7cm long, from one side of each brain they studied, while most IHC studies typically examine 5–48 μm sections. Usng an independent stereological measurement of the neurogenic volume of the human hippocampus [47], Spalding *et al.*'s estimation of 700 new neurons per day would equate to 5.2 neurons/mm^3/day. Now given that the half-life of DCX expression in the human SGZ is unknown, an extrapolation from rat data [48], suggests that 5.2 neurons/mm^3/day would equate to approximately 150 DCX^+ cells/mm^3. This figure is comparable to the 90–150 DCX^+ cells/mm^3 (0.45 ± 0.30 cells/mm^2 or one DCX^+ cell every 2 to 3 sections) found in the SGZ of 3/8 adults in the current study.

Therefore the results of SGZ studies utilising either exogenous markers such as ^{14}C [12] and BrdU [11] or endogenous IHC markers, may well be in agreement. At issue is whether the generation of 700 new neurons a day or 0.004% of the total granule cell population [12] is functionally significant. This estimate by Spalding and colleagues is approximately 10-fold lower than for rats (0.03%) [49] and mice (0.06%)[50] but is comparable to macaques (0.004 – 0.02%) [51, 52]. The marked differences between infants and adults in the current study suggests that in humans, the decline in neurogenesis with age is more rapid than in other mammals and that in adults, neurogenesis is functionally insignificant. Our conclusion is supported by a recent meta-analysis of hippocampal neurogenesis studies encompassing seven mammalian species, including humans, that suggested that age-related decline in humans is underestimated and that from middle age "neurogenesis occurs at relatively low, and perhaps negligible levels" [53].

Several hypotheses have been proposed to explain the differences in adult neurogenesis between humans and lower mammals. Ongoing neurogenesis in the adult SVZ may reflect the dominant role of olfaction in macro-osmic rodents [54] and sheep [55] compared with

micro-osmic primates [14, 56]. In the adult rodent SGZ neurogenesis may be necessary to erase ‘superfluous’ memories and ensure that the hippocampus remains receptive to new memories [7]. In infant humans, a similar process may be the basis of infantile amnesia [7]. Since, unlike lower mammals, primates including humans, do not rely on the hippocampus for remote memory recall or reconsolidation [57], functionally significant neurogenesis in the adult SGZ may be unnecessary.

Away from the SVZ and the SGZ, glial proliferation occurs at low levels even in healthy, adult human brains [58]. This has been largely attributed to oligodendrocyte precursor cell [59] and more recently, to microglia [23]. The rate of turnover of oligodendrocyte precursor cells in the adult human is unclear, in part due to the lack of a definitive marker. While NG2 (Chondroitin Sulphate Proteoglycan 4) has been used [59], this antigen is extremely sensitive to fixation, precluding its use in FFPE tissue. Our results demonstrate that within the adult human SVZ and SGZ the vast majority of proliferating cells are microglia and the degree of proliferation is similar to that noted in the surrounding brain parenchyma [23]. Similarly, Doorn *et al.* demonstrated that microglia are the predominant proliferating cells in the adult hippocampus [60]

Conclusions

Although commonly used,, PCNA is not aspecific marker of proliferation in postmortem human brain tissue. A combination of Ki67 and DCX immunoreactivity demonstrates that in humans, the density of proliferating cells, and neuroblasts in particular, declines markedly with age in the SVZ and SGZ and by four years of age is no greater than in the adjacent parenchyma. Although this low level of neurogenesis in neurologically normal adult humans suggests that any further reduction is unlikely to significantly contribute to the pathogenesis of neurodegenerative diseases the reported increases in neurogenesis in patients with conditions such as of Huntington’s disease [27] and epilepsy [61] suggests that therapeutic intervention to augment neurogenesis may be possible.

Supplementary Material

Refer to Web version on PubMed Central for supplementary material.

Acknowledgments

CVD, GTS and JJK designed the study. CVD and LSS contributed to data acquisition. DS, MLK and JJK contributed to provision of clinical and pathological data. CVD and GTS carried out data analysis and wrote the first draft. All authors contributed to manuscript review. The authors would like to thank the donors and their families for their kind gift that has allowed this research to be undertaken and the New South Wales Brain Tissue Resource Centre (NSW BTRC) and the NSW Department of Forensic Medicine for providing tissue samples. We would like to acknowledge Dr Louise Cole (Core Facilities Manager, Bosch Institute Advanced Microscopy Facility, The University of Sydney) for her support and assistance with the confocal microscopy. The NSW BTRC is part of the NSW Brain Bank Network and is supported by the University of Sydney, National Health and Medical Research Council (NHMRC), Schizophrenia Research Institute and the National Institutes of Alcoholism and Alcohol Abuse (NIAAA; R28 AA012725). This work was supported by the NIAAA (R28 AA012725) and the NHMRC (grant #605210).

Abbreviations

CC	Corpus callosum
CN	Caudate nucleus
DCX	Doublecortin
EGFR	Epidermal growth factor receptor
FFPE	Formalin-fixed paraffin-embedded
GCL	Granule cell layer
GFAP	Glial fibrillary acidic protein
Iba1	ionized calcium binding adaptor molecule 1
IHC	Immunohistochemistry
PCNA	Proliferating cell nuclear antigen
PML	Polymorphic layer
RMS	Rostral migratory stream
SFG	Superior frontal gyrus
SGZ	Subgranular zone
SVZ	Subventricular zone

References

1. Falk A, Frisen J. New neurons in old brains. Ann Med. 2005; 37:480–6. [PubMed: 16278161]
2. Taylor CJ, Jhaveri DJ, Bartlett PF. The therapeutic potential of endogenous hippocampal stem cells for the treatment of neurological disorders. Frontiers in cellular neuroscience. 2013; 7:5. [PubMed: 23372544]
3. Capilla-Gonzalez V, Herranz-Perez V, Garcia-Verdugo JM. The aged brain: genesis and fate of residual progenitor cells in the subventricular zone. Frontiers in cellular neuroscience. 2015; 9:365. [PubMed: 26441536]
4. Mouret A, Murray K, Lledo PM. Centrifugal drive onto local inhibitory interneurons of the olfactory bulb. Ann N Y Acad Sci. 2009; 1170:239–54. [PubMed: 19686142]
5. Nissant A, Bardy C, Katagiri H, Murray K, Lledo PM. Adult neurogenesis promotes synaptic plasticity in the olfactory bulb. Nat Neurosci. 2009; 12:728–30. [PubMed: 19412168]
6. van Praag H, Schinder AF, Christie BR, Toni N, Palmer TD, Gage FH. Functional neurogenesis in the adult hippocampus. Nature. 2002; 415:1030–4. [PubMed: 11875571]
7. Akers KG, Martinez-Canabal A, Restivo L, Yiu AP, De Cristofaro A, Hsiang HL, Wheeler AL, Guskjolen A, Niibori Y, Shoji H, Ohira K, Richards BA, Miyakawa T, Josselyn SA, Frankland PW. Hippocampal neurogenesis regulates forgetting during adulthood and infancy. Science. 2014; 344:598–602. [PubMed: 24812394]
8. Curtis MA, Kam M, Nannmark U, Anderson MF, Axell MZ, Wikkelso C, Holtas S, van Roon-Mom WM, Bjork-Eriksson T, Nordborg C, Frisen J, Dragunow M, Faull RL, Eriksson PS. Human neuroblasts migrate to the olfactory bulb via a lateral ventricular extension. Science. 2007; 315:1243–9. [PubMed: 17303719]

9. Couillard-Despres S, Winner B, Schaubeck S, Aigner R, Vroemen M, Weidner N, Bogdahn U, Winkler J, Kuhn HG, Aigner L. Doublecortin expression levels in adult brain reflect neurogenesis. Eur J Neurosci. 2005; 21:1–14. [PubMed: 15654838]
10. Sanai N, Nguyen T, Ihrie RA, Mirzadeh Z, Tsai HH, Wong M, Gupta N, Berger MS, Huang E, Garcia-Verdugo JM, Rowitch DH, Alvarez-Buylla A. Corridors of migrating neurons in the human brain and their decline during infancy. Nature. 2011 Sep 28; 478(7369):382–6. [PubMed: 21964341]
11. Knoth R, Singec I, Ditter M, Pantazis G, Capetian P, Meyer RP, Horvat V, Volk B, Kempermann G. Murine features of neurogenesis in the human hippocampus across the lifespan from 0 to 100 years. PLoS One. 2010; 5:e8809. [PubMed: 20126454]
12. Spalding KL, Bergmann O, Alkass K, Bernard S, Salehpour M, Huttner HB, Bostrom E, Westerlund I, Vial C, Buchholz BA, Possnert G, Mash DC, Druid H, Frisen J. Dynamics of hippocampal neurogenesis in adult humans. Cell. 2013; 153:1219–27. [PubMed: 23746839]
13. Ernst A, Alkass K, Bernard S, Salehpour M, Perl S, Tisdale J, Possnert G, Druid H, Frisen J. Neurogenesis in the striatum of the adult human brain. Cell. 2014; 156:1072–83. [PubMed: 24561062]
14. Bergmann O, Liebl J, Bernard S, Alkass K, Yeung MS, Steier P, Kutschera W, Johnson L, Landen M, Druid H, Spalding KL, Frisen J. The age of olfactory bulb neurons in humans. Neuron. 2012; 74:634–9. [PubMed: 22632721]
15. Lyck L, Dalmau I, Chemnitz J, Finsen B, Schroder HD. Immunohistochemical markers for quantitative studies of neurons and glia in human neocortex. J Histochem Cytochem. 2008; 56:201–21. [PubMed: 17998570]
16. Sutherland GT, Sheahan PJ, Matthews J, Dennis CV, Sheedy DS, McCrossin T, Curtis MA, Kril JJ. The effects of chronic alcoholism on cell proliferation in the human brain. Exp Neurol. 2013; 247:9–18. [PubMed: 23541433]
17. Quinones-Hinojosa A, Sanai N, Soriano-Navarro M, Gonzalez-Perez O, Mirzadeh Z, Gil-Perotin S, Romero-Rodriguez R, Berger MS, Garcia-Verdugo JM, Alvarez-Buylla A. Cellular composition and cytoarchitecture of the adult human subventricular zone: a niche of neural stem cells. J Comp Neurol. 2006; 494:415–34. [PubMed: 16320258]
18. Doetsch F, Petreanu L, Caille I, Garcia-Verdugo JM, Alvarez-Buylla A. EGF converts transit-amplifying neurogenic precursors in the adult brain into multipotent stem cells. Neuron. 2002; 36:1021–34. [PubMed: 12495619]
19. Menezes JR, Luskin MB. Expression of neuron-specific tubulin defines a novel population in the proliferative layers of the developing telencephalon. J Neurosci. 1994; 14:5399–416. [PubMed: 8083744]
20. Pixley SK, de Vellis J. Transition between immature radial glia and mature astrocytes studied with a monoclonal antibody to vimentin. Brain Res. 1984; 317:201–9. [PubMed: 6383523]
21. Middeldorp J, Hol EM. GFAP in health and disease. Prog Neurobiol. 2011; 93:421–43. [PubMed: 21219963]
22. Ito D, Imai Y, Ohsawa K, Nakajima K, Fukuuchi Y, Kohsaka S. Microglia-specific localisation of a novel calcium binding protein, Iba1. Brain Res Mol Brain Res. 1998; 57:1–9. [PubMed: 9630473]
23. Dennis CV, Sheahan PJ, Graeber MB, Sheedy DL, Kril JJ, Sutherland GT. Microglial proliferation in the brain of chronic alcoholics with hepatic encephalopathy. Metab Brain Dis. 2014; 29:1027–39. [PubMed: 24346482]
24. Marshall CA, Novitch BG, Goldman JE. Olig2 directs astrocyte and oligodendrocyte formation in postnatal subventricular zone cells. J Neurosci. 2005; 25:7289–98. [PubMed: 16093378]
25. Menn B, Garcia-Verdugo JM, Yaschine C, Gonzalez-Perez O, Rowitch D, Alvarez-Buylla A. Origin of oligodendrocytes in the subventricular zone of the adult brain. J Neurosci. 2006; 26:7907–18. [PubMed: 16870736]
26. Wang C, Liu F, Liu YY, Zhao CH, You Y, Wang L, Zhang J, Wei B, Ma T, Zhang Q, Zhang Y, Chen R, Song H, Yang Z. Identification and characterization of neuroblasts in the subventricular zone and rostral migratory stream of the adult human brain. Cell Res. 2011 Nov; 21(11):1534–50. [PubMed: 21577236]

27. Curtis MA, Penney EB, Pearson AG, van Roon-Mom WM, Butterworth NJ, Dragunow M, Connor B, Faull RL. Increased cell proliferation and neurogenesis in the adult human Huntington's disease brain. Proc Natl Acad Sci U S A. 2003; 100:9023–7. [PubMed: 12853570]
28. Curtis MA, Penney EB, Pearson J, Dragunow M, Connor B, Faull RL. The distribution of progenitor cells in the subependymal layer of the lateral ventricle in the normal and Huntington's disease human brain. Neuroscience. 2005; 132:777–88. [PubMed: 15837138]
29. van den Berge SA, van Strien ME, Korecka JA, Dijkstra AA, Sluijs JA, Kooijman L, Eggers R, De Filippis L, Vescovi AL, Verhaagen J, van de Berg WD, Hol EM. The proliferative capacity of the subventricular zone is maintained in the parkinsonian brain. Brain. 2011; 134:3249–63. [PubMed: 22075520]
30. Funato H, Yoshimura M, Ito Y, Okeda R, Ihara Y. Proliferating cell nuclear antigen (PCNA) expressed in human leptomeninges. J Histochem Cytochem. 1996; 44:1261–5. [PubMed: 8918901]
31. Ino H, Chiba T. Expression of proliferating cell nuclear antigen (PCNA) in the adult and developing mouse nervous system. Brain Res Mol Brain Res. 2000; 78:163–74. [PubMed: 10891596]
32. Stoimenov I, Helleday T. PCNA on the crossroad of cancer. Biochem Soc Trans. 2009; 37:605–13. [PubMed: 19442257]
33. Zessin PJ, Sporbert A, Heilemann M. PCNA appears in two populations of slow and fast diffusion with a constant ratio throughout S-phase in replicating mammalian cells. Sci Rep. 2016; 6:18779. [PubMed: 26758689]
34. Verwer RW, Sluiter AA, Balesar RA, Baayen JC, Noske DP, Dirven CM, Wouda J, van Dam AM, Lucassen PJ, Swaab DF. Mature astrocytes in the adult human neocortex express the early neuronal marker doublecortin. Brain. 2007; 130:3321–35. [PubMed: 18055496]
35. Klempin F, Kronenberg G, Cheung G, Kettenmann H, Kempermann G. Properties of doublecortin-(DCX)-expressing cells in the piriform cortex compared to the neurogenic dentate gyrus of adult mice. PLoS One. 2011; 6:e25760. [PubMed: 22022443]
36. Worlitzer MM, Viel T, Jacobs AH, Schwamborn JC. The majority of newly generated cells in the adult mouse substantia nigra express low levels of Doublecortin, but their proliferation is unaffected by 6-OHDA-induced nigral lesion or Minocycline-mediated inhibition of neuroinflammation. Eur J Neurosci. 2013; 38:2684–92. [PubMed: 23734736]
37. Boekhoorn K, Joels M, Lucassen PJ. Increased proliferation reflects glial and vascular-associated changes, but not neurogenesis in the presenile Alzheimer hippocampus. Neurobiol Dis. 2006; 24:1–14. [PubMed: 16814555]
38. Ihrie RA, Alvarez-Buylla A. Lake-front property: a unique germinal niche by the lateral ventricles of the adult brain. Neuron. 2011; 70:674–86. [PubMed: 21609824]
39. Kohler SJ, Williams NI, Stanton GB, Cameron JL, Greenough WT. Maturation time of new granule cells in the dentate gyrus of adult macaque monkeys exceeds six months. Proc Natl Acad Sci U S A. 2011; 108:10326–31. [PubMed: 21646517]
40. Galvez-Contreras AY, Quinones-Hinojosa A, Gonzalez-Perez O. The role of EGFR and ErbB family related proteins in the oligodendrocyte specification in germinal niches of the adult mammalian brain. Frontiers in cellular neuroscience. 2013; 7:258. [PubMed: 24381541]
41. Roelofs RF, Fischer DF, Houtman SH, Sluijs JA, Van Haren W, Van Leeuwen FW, Hol EM. Adult human subventricular, subgranular, and subpial zones contain astrocytes with a specialized intermediate filament cytoskeleton. Glia. 2005; 52:289–300. [PubMed: 16001427]
42. van den Berge SA, Middeldorp J, Zhang CE, Curtis MA, Leonard BW, Mastroeni D, Voorn P, van de Berg WD, Huitinga I, Hol EM. Longterm quiescent cells in the aged human subventricular neurogenic system specifically express GFAP-delta. Aging Cell. 2010; 9:313–26. [PubMed: 20121722]
43. Sohn J, Orosco L, Guo F, Chung SH, Bannerman P, Mills Ko E, Zarbalis K, Deng W, Pleasure D. The subventricular zone continues to generate corpus callosum and rostral migratory stream astroglia in normal adult mice. J Neurosci. 2015; 35:3756–63. [PubMed: 25740506]

44. Malik SZ, Lewis M, Isaacs A, Haskins M, Van Winkle T, Vite CH, Watson DJ. Identification of the rostral migratory stream in the canine and feline brain. PLoS One. 2012; 7:e36016. [PubMed: 22606243]
45. Alonso M, Ortega-Perez I, Grubb MS, Bourgeois JP, Charneau P, Lledo PM. Turning astrocytes from the rostral migratory stream into neurons: a role for the olfactory sensory organ. J Neurosci. 2008; 28:11089–102. [PubMed: 18945916]
46. Gritti A, Bonfanti L, Doetsch F, Caille I, Alvarez-Buylla A, Lim DA, Galli R, Verdugo JM, Herrera DG, Vescovi AL. Multipotent neural stem cells reside into the rostral extension and olfactory bulb of adult rodents. J Neurosci. 2002; 22:437–45. [PubMed: 11784788]
47. Boldrini M, Santiago AN, Hen R, Dwork AJ, Rosoklija GB, Tamir H, Arango V, John Mann J. Hippocampal granule neuron number and dentate gyrus volume in antidepressant-treated and untreated major depression. Neuropsychopharmacology. 2013; 38:1068–77. [PubMed: 23303074]
48. Brown J, Cooper-Kuhn CM, Kempermann G, Van Praag H, Winkler J, Gage FH, Kuhn HG. Enriched environment and physical activity stimulate hippocampal but not olfactory bulb neurogenesis. Eur J Neurosci. 2003; 17:2042–6. [PubMed: 12786970]
49. Cameron HA, McKay RD. Adult neurogenesis produces a large pool of new granule cells in the dentate gyrus. J Comp Neurol. 2001; 435:406–17. [PubMed: 11406822]
50. Kempermann G, Kuhn HG, Gage FH. Genetic influence on neurogenesis in the dentate gyrus of adult mice. Proc Natl Acad Sci U S A. 1997; 94:10409–14. [PubMed: 9294224]
51. Jabes A, Lavenex PB, Amaral DG, Lavenex P. Quantitative analysis of postnatal neurogenesis and neuron number in the macaque monkey dentate gyrus. Eur J Neurosci. 2010; 31:273–85. [PubMed: 20074220]
52. Kornack DR, Rakic P. Continuation of neurogenesis in the hippocampus of the adult macaque monkey. Proc Natl Acad Sci U S A. 1999; 96:5768–73. [PubMed: 10318959]
53. Lazic SE. Modeling hippocampal neurogenesis across the lifespan in seven species. Neurobiol Aging. 2012; 33:1664–71. [PubMed: 21621300]
54. Mak GK, Enwere EK, Gregg C, Pakarainen T, Poutanen M, Huhtaniemi I, Weiss S. Male pheromone-stimulated neurogenesis in the adult female brain: possible role in mating behavior. Nat Neurosci. 2007; 10:1003–11. [PubMed: 17603480]
55. Low VF, Faull RL, Bennet L, Gunn AJ, Curtis MA. Neurogenesis and progenitor cell distribution in the subgranular zone and subventricular zone of the adult sheep brain. Neuroscience. 2013; 244:173–87. [PubMed: 23587842]
56. Kornack DR, Rakic P. Cell proliferation without neurogenesis in adult primate neocortex. Science. 2001; 294:2127–30. [PubMed: 11739948]
57. Hattori S, Chen L, Weiss C, Disterhoft JF. Robust hippocampal responsivity during retrieval of consolidated associative memory. Hippocampus. 2015; 25:655–69. [PubMed: 25515308]
58. Bhardwaj RD, Curtis MA, Spalding KL, Buchholz BA, Fink D, Bjork-Eriksson T, Nordborg C, Gage FH, Druid H, Eriksson PS, Frisen J. Neocortical neurogenesis in humans is restricted to development. Proc Natl Acad Sci U S A. 2006; 103:12564–8. [PubMed: 16901981]
59. Geha S, Pallud J, Junier MP, Devaux B, Leonard N, Chassoux F, Chneiweiss H, Daumas-Duport C, Varlet P. NG2+/Olig2+ cells are the major cycle-related cell population of the adult human normal brain. Brain Pathol. 2010; 20:399–411. [PubMed: 19486010]
60. Doorn KJ, Drukarch B, van Dam AM, Lucassen PJ. Hippocampal proliferation is increased in presymptomatic Parkinson's disease and due to microglia. Neural plasticity. 2014; 2014:959154. [PubMed: 25197578]
61. Liu YW, Curtis MA, Gibbons HM, Mee EW, Bergin PS, Teoh HH, Connor B, Dragunow M, Faull RL. Doublecortin expression in the normal and epileptic adult human brain. Eur J Neurosci. 2008; 28:2254–65. [PubMed: 19046368]

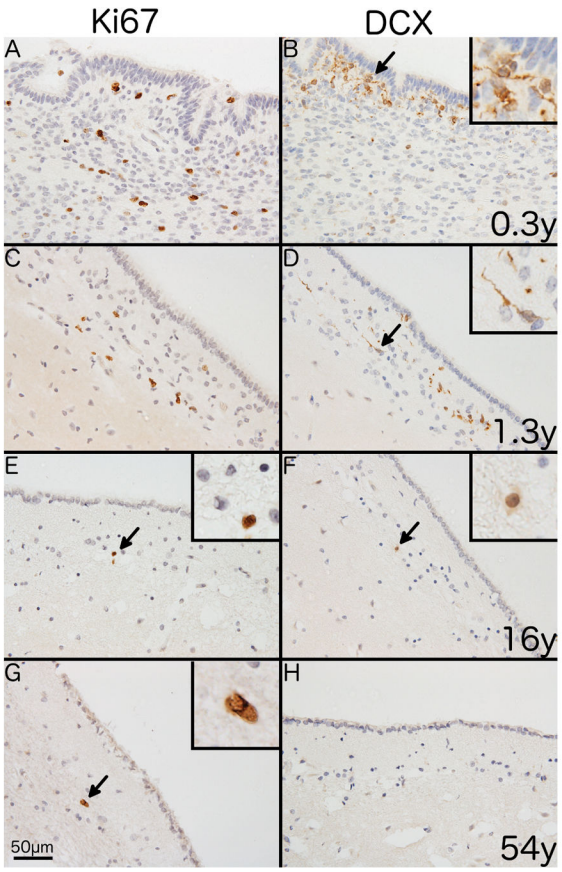

Fig. 1. Immunostaining of endogenous markers of proliferation and neurogenesis in the human SVZ

Representative photomicrographs showing differences in immunostaining for Ki67 (A, C, E and G) and DCX (B, D, F and H) with age. Immunostaining of the SVZ from a 0.3 year-old individual shows (A) numerous $Ki67^+$ cells with a nuclear staining pattern and (B) clusters of DCX^+ cells with a combination of somatic and dendritic staining. A similar pattern is shown in a 1.3 year-old individual for both Ki67 (C) and DCX (D). A 16 year-old individual shows (E) a single $Ki67^+$ cell (black arrow) in the SVZ and (F) shows a single DCX^+ cell (black arrow) with weak somatic staining. A 54 year-old individual shows (G) a single $Ki67^+$ cell (black arrow) and (H) no DCX^+ cells. 400x magnification. Scale bar = 50μm. Insets show digital enlargement of immunopositive cells.

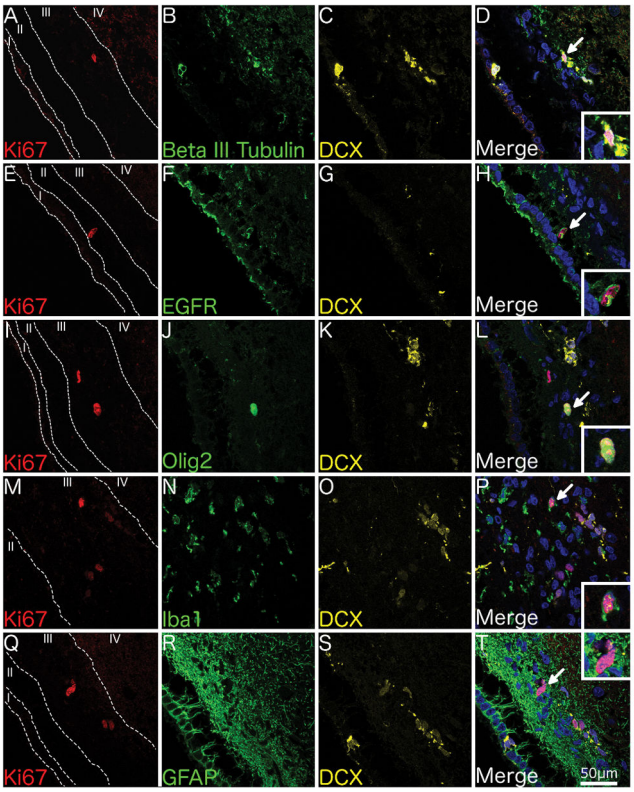

Fig. 2. Phenotype of proliferating cells in the juvenile SVZ

Confocal micrographs of the SVZ from a 1 year-old individual shows Ki67^{+} cells co-localising with the immature neuronal marker beta III tubulin and the neuroblast marker DCX (A–D), the transit-amplifier marker EGFR (E–H), the oligodendrocytic marker Olig2 (I–L), the microglial marker Iba1 (M–P) but not the astrocytic marker GFAP (Q–T). 400x Magnification. Scale bar = 50μm. Insets show higher magnification of Ki67^{+} cells.

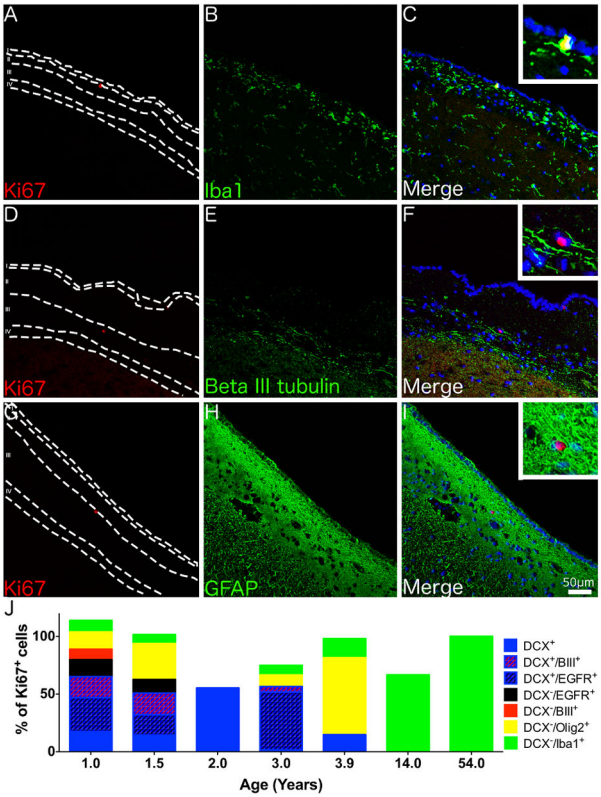

Fig. 3. Phenotype of proliferating cells in the adult SVZ

Confocal micrographs of the SVZ from a 54 year-old individual shows Ki67$^+$ cells co-localising with the microglial marker Iba1 (A–C) but not the immature neuronal marker beta III tubulin (D–F) or the astrocytic marker GFAP (G–I). (J) A graph displaying the number of Ki67$^+$ cells co-localising with different cell specific markers in the SVZ across a range of ages, note as quantification was performed on serial tissue sections totals could exceed or be less than 100%. (A–I) Magnification = 200x, Insets - 600x. Scale bar = 50 μm.

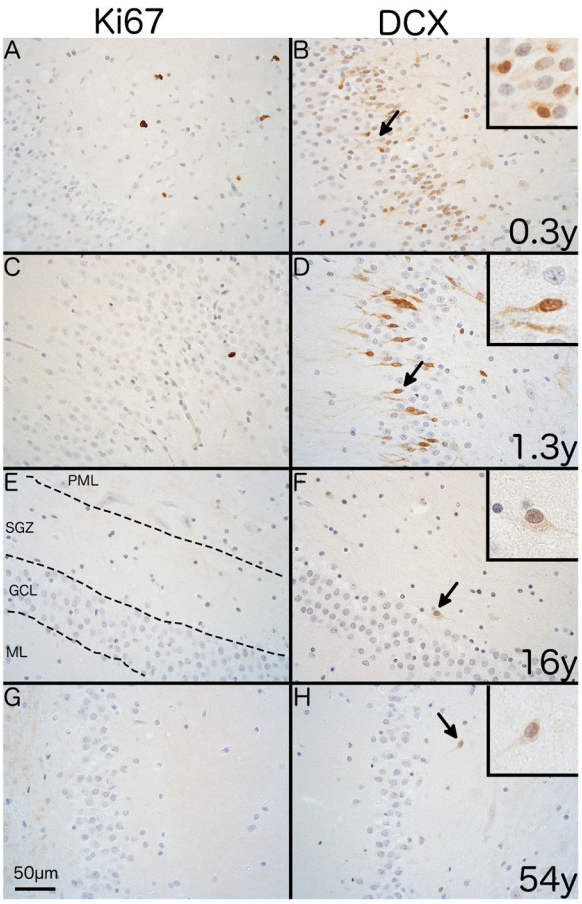

Fig. 4. Immunostaining of endogenous markers of proliferation and neurogenesis in the human SGZ

Representative photomicrographs showing differences in immunostaining for Ki67 and DCX with age with the polymorphic layer to the right side in all images. Immunostaining shows the SGZ of a 0.3 year-old individual with (A) numerous $Ki67^+$ cells with a nuclear staining pattern and (B) abundant DCX^+ cells with predominantly somatic staining. A 1.3 year-old shows (C) a single $Ki67^+$ cell and (D) numerous DCX^+ cells with predominantly cytoplasmic staining. A16 year-old individual shows no $Ki67^+$ cells (E) and a single DCX^+ cell with dendritic and somatic staining (arrow). A 54 year-old individual shows the same pattern for both Ki67 (G) and DCX (H) as the 16 year-old individual. 400x magnification. Scale bar = 50μm.

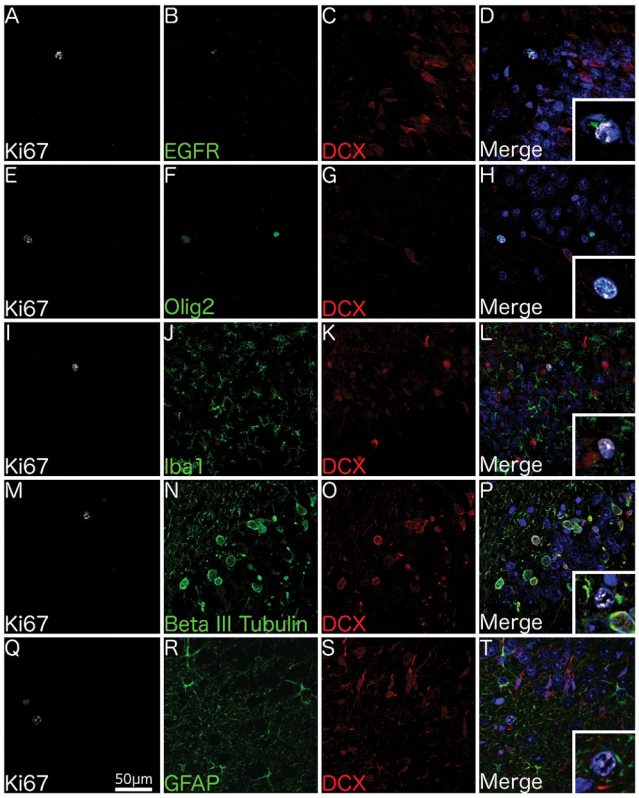

Fig. 5. Phenotype of proliferating cells in the juvenile SGZ

Confocal micrographs of the SGZ from a 1 year-old individual shows $Ki67^+$ cells co-localising with the transit-amplifier marker EGFR (A–D), the oligodendrocytic marker Olig2 (E–H), but not the microglial marker Iba1 (I–L), the immature neuronal marker beta III tubulin (M–P) or the astrocytic marker GFAP (Q–T). 400x Magnification. Scale bar = 50 μm. Insets show digital enlargement of $Ki67^+$ cells.

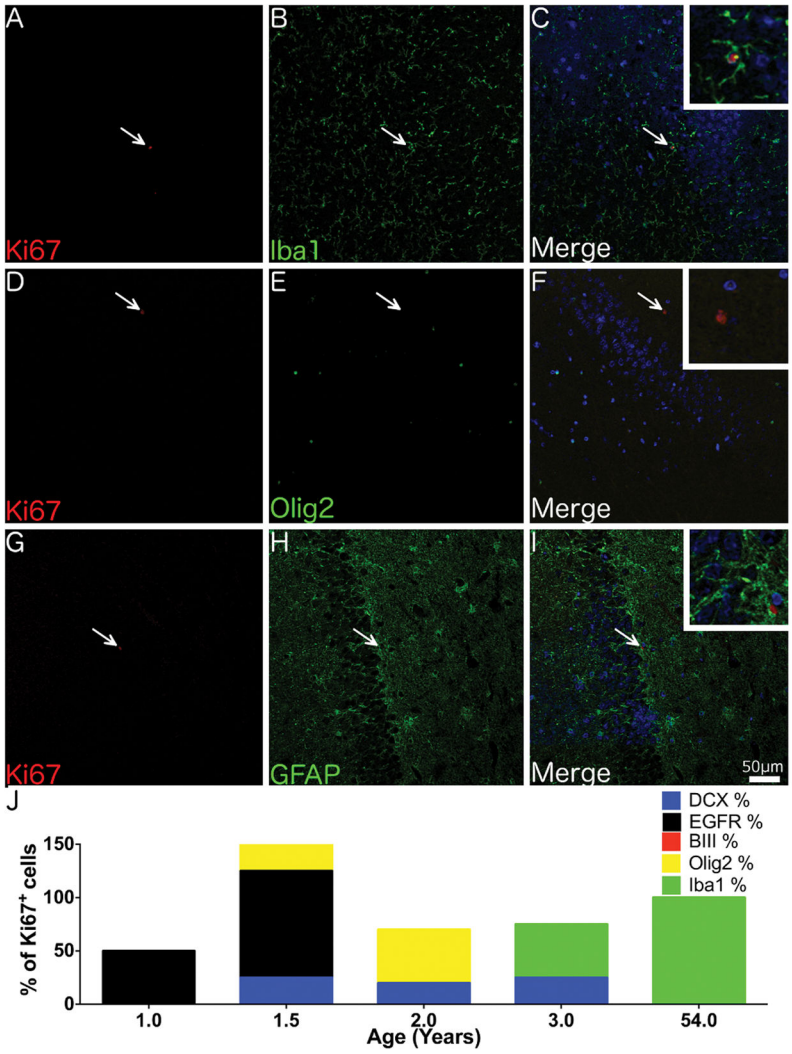

Fig. 6. Phenotype of proliferating cells in the adult SGZ

Confocal micrographs of the SGZ from a 54 year-old individual shows Ki67$^+$ cells co-localising with the microglial marker Iba1 (A–C) but not the immature neuronal marker beta III tubulin (D–F) or the astrocytic marker GFAP (G–I). (J) A graph displaying the number of Ki67$^+$ cells co-localising with different cell specific markers in the SGZ across a range of ages. N.B. as quantification was performed on serial tissue sections totals could exceed or be less than 100%. (A–I) Magnification = 200x. Insets at 600x magnification. Scale bar = 50 μm.

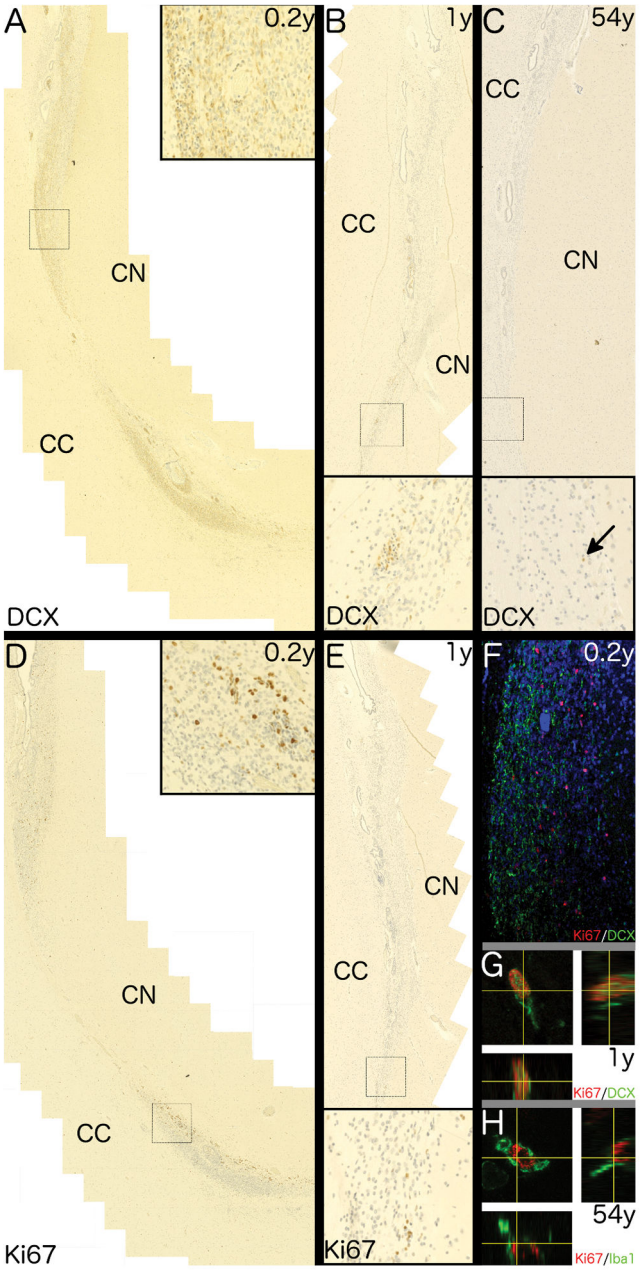

Fig. 7. Characterisation of the RMS

Photomicrographs show traces of the rostral migratory stream with distinctive ependymal islets extending rostrally from and confluent with the frontal horn of the lateral ventricle between the corpus callosum (CC) and head of the caudate nucleus (CN). Higher magnifications of regions corresponding to black rectangles are shown in insets. Collages of overlapping fields show DCX^+ cells throughout the dorsomedial portion of the RMS in a (A) 0.2 year-old and (B) one year-old brain but only a single DCX^+ cell (nuclear) in the (C) 54 year-old. (D – E) $Ki67^+$ cells are seen in ventrolateral portion of the RMS in (D) 0.2 year-old but markedly fewer $Ki67^+$ cells within the RMS of (E) a one year-old. (F) a confocal micrograph showing the disparity of Ki67 (red) and DCX (green) within the RMS of a 0.2

year-old individual. Orthogonal projections of z-stacks show (G) a rare $Ki67^+/DCX^+$ cells in the infant RMS whilst and (H) a $Ki67^+$ cellsin the adult RMS co-positive for the microglia marker, Iba1.

Neuropathol Appl Neurobiol. Author manuscript; available in PMC 2017 December 01.

Table 1

Details of cases included in this study

Case ID	Classification	Sex	Age (Years)	PMI (Hours)	Cause of Death	Brain pH	Immunofluorescence analysis performed
1	Juvenile	Male	0.2	44	Undetermined	n/a	No
2	Juvenile	Female	0.3	52	Undetermined	n/a	No
3	Juvenile	Male	1.0	18	Respiratory	n/a	Yes
4	Juvenile	Female	1.0	47	Undetermined	n/a	No
5	Juvenile	Male	1.0	46	Drowning	n/a	No
6	Juvenile	Female	1.3	32	Infection	n/a	Yes
7	Juvenile	Male	1.3	20	Respiratory	n/a	No
8	Juvenile	Male	2.0	60	Drowning	n/a	Yes
9	Juvenile	Male	2.5	90	Drowning	n/a	No
10	Juvenile	Female	3.0	43	Drowning	n/a	Yes
11	Juvenile	Female	3.9	35	Respiratory	n/a	Yes
12	Juvenile	Female	7.0	41	Respiratory	n/a	No
13	Juvenile	Male	7.0	15	Respiratory	n/a	No
14	Juvenile	Male	14	18	Trauma	n/a	Yes
15	Juvenile	Female	16	18	Drowning	n/a	No
16	Adult	Male	24	43	Cardiac	6.57	No
17	Adult	Female	29	40	Cardiac	6.83	No
18	Adult	Male	37	15	Cardiac	6.46	No
19	Adult	Male	43	66	Respiratory	6.57	No
20	Adult	Male	47	38	Cardiac	6.2	No
21	Adult	Female	49	15	Cardiac	6.97	No
22	Adult	Male	54	28	Cardiac	6.38	Yes
23	Adult	Male	59	29	Respiratory	6.61	No